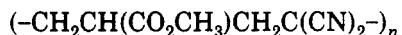


# Communications to the Editor

## Three-Dimensional Nuclear Magnetic Resonance Determination of Polymer Chain Conformation

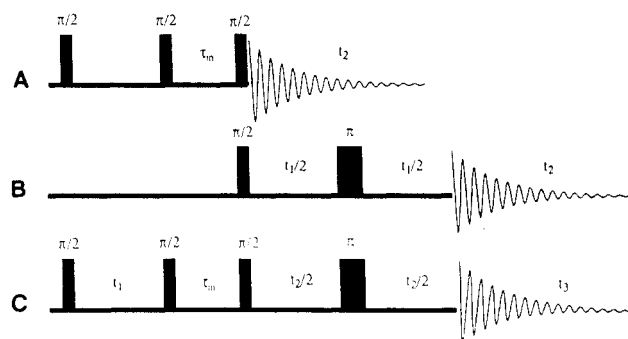
The relationship between the physical, mechanical, and electrical properties of polymers and their chain conformations has been an area of intense interest and investigation.<sup>1,2</sup> Relating the properties of polymers on a molecular/atomic level to the macroscopic properties is limited by the relatively small number of techniques that are able to probe polymer structure at the molecular level. Among these, NMR has been successful because the relaxation is sensitive to interactions over a few angstroms and the through-bond  $J$  couplings depend on the conformation over a distance scale of 2-5 bonds.<sup>3</sup> The  $J$  couplings have been extensively used for conformational analysis in small molecules, since the magnitude of the  $J$  couplings depends on the dihedral angle between the coupled protons. The introduction of two-dimensional (2D)  $J$ -resolved spectroscopy has greatly extended the number of molecules that can be analyzed due to the dramatic increase in resolution that accompanies the change from 1D to 2D NMR.<sup>4,5</sup> To measure  $J$  couplings by 2D  $J$ -resolved spectroscopy, the chemical shifts of the protons of interest must be sufficiently separated that the  $J$  couplings can be resolved in the second frequency dimension. This technique has been used in polymers<sup>6,7</sup> but is lacking in general utility due to the large apparent line widths found for many high polymers in solution. The complex microstructure of polymers, principally due to stereochemical isomerism, leads to inhomogeneously broadened lines that typically overlap even at the highest magnetic fields.<sup>1</sup>

Polymer chain conformation depends not only on the monomer sequence, composition, and microstructure but also on the solvent, and the behavior of polymer films can in some cases be related to these conformational effects.<sup>8</sup> We are investigating solvent effects on the conformation of poly(vinyl acetate/vinylidene cyanide) both in solution and in films. Poly(vinyl acetate/vinylidene cyanide) is a highly alternating amorphous copolymer with dem-



poly(vinyl acetate/vinylidene cyanide)

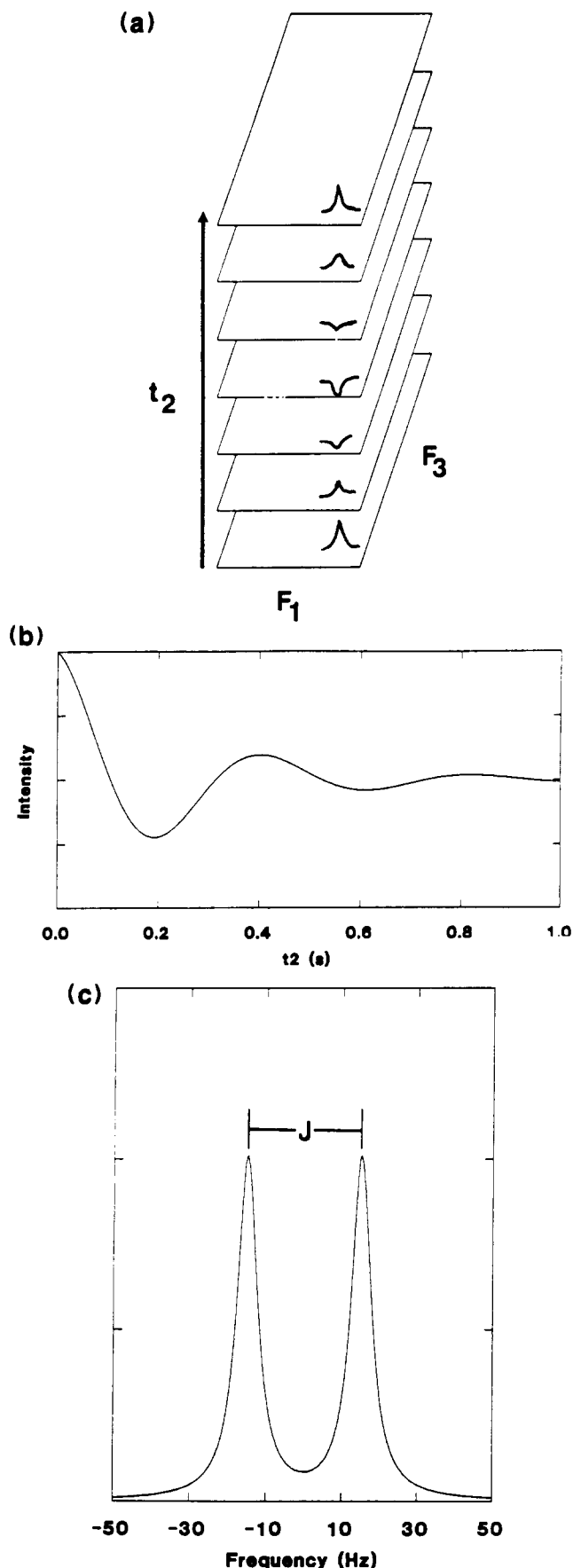
onstrated piezoelectric properties.<sup>9-12</sup> Both the piezoelectricity and the thermal behavior of poly(vinyl acetate/vinylidene cyanide) films depend on the casting solvent and sample history.<sup>12</sup> Piezoelectricity depends on the orientation of dipoles, so the effect of solvent on chain conformation may be particularly important. Here we investigate the solution conformation of poly(vinyl acetate/vinylidene cyanide) in DMF solution by measuring the through-bond  $J$  coupling constants along the main chain of the polymer. The magnitude of the methine-methylene coupling depends on the dihedral angle between the coupled vicinal protons and provides a measure of the average chain conformation.<sup>1,3-5</sup> The combination of broad polymer resonances and overlap with the residual solvent line prohibits measurement of chain conformation by the usual 2D NMR methods. In this study we explore the use of 3D NMR<sup>14-16</sup> as a tool for measuring  $J$  couplings in polymers and determining polymer chain conformation.



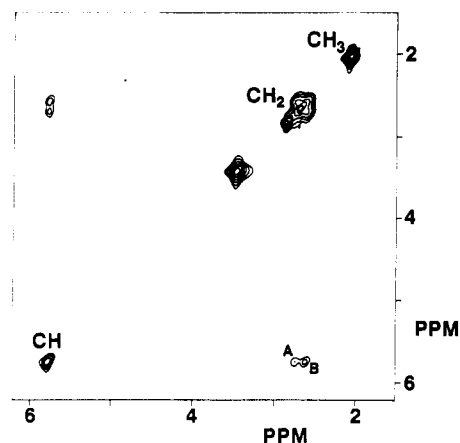
**Figure 1.** Pulse sequence diagrams for (A) 2D nuclear Overhauser effect spectroscopy, (B) 2D  $J$ -resolved spectroscopy, and (C) 3D NOE/ $J$ -resolved spectroscopy.

Figure 1 shows the pulse sequence diagram for 2D nuclear Overhauser effect (NOE) spectroscopy,<sup>17</sup> 2D  $J$ -resolved spectroscopy,<sup>18</sup> and the combination sequence for 3D NOE/ $J$ -resolved spectroscopy. There are three independent time variables in the new pulse sequence that are related by Fourier transforms to three independent frequency variables. Figure 2 schematically illustrates how  $J$  coupling information is obtained from the 3D NOE/ $J$ -resolved spectra. The data set consists of a series of 2D spectra that differ only in the delay  $t_2$ , a time period during which the spins precess under the influence of the homonuclear  $J$  coupling. Each of the data sets is transformed along the  $F_1/F_3$  axes to give a series of 2D NOE spectra in which the peak intensities are modulated during the  $t_2$  delay (Figure 2a). The cross-peak intensities of interest are extracted to form a free induction decay (Figure 2b) and Fourier transformed along the  $t_2$  dimension (Figure 2c) to give the  $J$  coupling pattern. The final spectrum consists of peak intensities as a function of the three frequency axes. These data are hard to visualize, so it is more convenient to examine either contour plots of projections along two frequency axes or slices through the 3D NMR data set. The primary advantage of the 3D experiment relative to the 2D experiment is resolution. The  $J$  coupling pattern can be obtained from either the diagonal or cross peaks in the 3D experiment; this greatly increases the probability that the peaks of interest will be resolved for the  $J$  coupling analysis.

The use of 3D NMR for  $J$  coupling measurements has been reported for small molecules by using through-bond correlations (COSY) in the  $F_1$  and  $F_3$  dimensions.<sup>16</sup> This approach is not generally successful in polymers because of the large inhomogeneous line widths, so another is developed. The 3D NOE/ $J$ -resolved experiment is better suited to polymer studies because the through-space dipolar interactions are more efficient at generating cross peaks than are the through-bond interactions,<sup>6</sup> and remote cross peaks (from protons not connected by through-bond coupling) can also be analyzed. COSY experiments are also more sensitive to digital resolution,<sup>4,5</sup> which is necessarily limited in the 3D NMR experiments in order to decrease the size of the data matrix and the experimental acquisition time. A more complete discussion of 3D NOE/ $J$ -resolved and 3D COSY/ $J$ -resolved experiments will be reported elsewhere.<sup>19</sup>



**Figure 2.** Schematic diagram showing the processing of a 3D data matrix. The data is collected as a function of the  $t_1$ ,  $t_2$ , and  $t_3$  time variables and subjected to a double Fourier transform along the  $F_1/F_3$  frequency axes. The intensity modulations of the cross peaks are measured, and an interferogram is constructed from the modulation (b). Fourier transformation with respect to  $t_2$  (c) gives the  $J$  coupling pattern for each resolved cross peak.



**Figure 3.** 2D NOE spectrum of 2 wt % poly(vinyl acetate/vinylidene cyanide) acquired at 500 MHz with a mixing time of 0.5 s in DMF- $d_7$  at 20 °C. The diagonal methine, methylene, and methyl proton resonances are labeled, and the cross peaks marked A and B are discussed in the text. A solvent impurity (H<sub>2</sub>O) is observed at 3.5 ppm.

Figure 3 shows the 2D NOE spectrum of a 2 wt % solution of poly(vinyl acetate/vinylidene cyanide) in deuterated DMF at 500 MHz. The spectrum was obtained with a mixing time of 0.5 s and is the first in the hypercomplex, phase-sensitive<sup>20</sup> 3D data set. The data were acquired as 128 (complex)  $\times$  32  $\times$  256 (complex) data points and processed to a final size of 256  $\times$  64  $\times$  256 (real) points with sweep widths in the  $F_1$ ,  $F_2$ , and  $F_3$  dimensions of 4000, 100, and 4000 Hz. The spectra were processed with 4-Hz line broadening in the  $F_1$  and  $F_3$  dimensions and with a skewed sine-bell apodization along the  $F_2$  dimension. The delay between acquisitions was decreased to 1.5 s to reduce the time of the experiment (30 h).

There are four resonances of interest that can be assigned to the methine (5.7 ppm), the two groups of methylene protons (2.6 and 2.4 ppm), and the methoxyl protons (1.8 ppm) of the vinyl acetate. The analysis of the  $J$  couplings to the methylene protons along the diagonal is complicated by overlap with the residual line from the DMF solvent. The conformation could be analyzed in principle from the multiplicity of the methine protons. However, the methine proton coupling pattern is extremely complex and may contain up to eight closely spaced lines (from coupling to four protons). The fine structure of such complex coupling patterns is difficult to measure with broad lines, and 2D  $J$ -resolved experiments were not successful (not shown).

The  $J$  coupling information is obtained by Fourier transformation of the modulation of the methine-methylene cross peaks, marked A and B in Figure 3, as a function of the  $t_2$  time delay. This cross peak results from magnetization that is labeled at the methine frequency during the  $t_1$  interval and is transferred to the methylene protons via through-space dipolar interactions during the mixing time ( $\tau_m$ ) (Figure 1C). The  $\pi/2$  pulse following the mixing time returns the magnetization to the transverse plane where it evolves under the influence of the homonuclear  $J$  coupling and where it is finally detected during the  $t_3$  period. Since the magnetization evolved during the  $t_2$  period at the methylene proton frequency, Fourier transformation of the cross-peak modulation yields the methylene  $J$  coupling pattern. These results are shown in parts A and B of Figure 4. The methylene protons can be split by the coupling to the geminal and vicinal neighboring protons. The geminal coupling is fixed by the geometry of the system, but the magnitude of the vicinal coupling depends on the chain conformation. Figure 4A shows that the downfield proton is split by the 14-Hz gem-

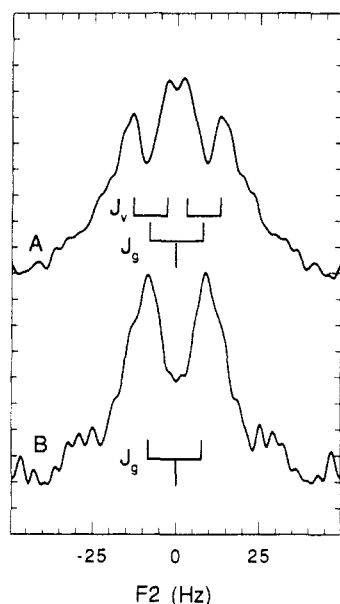


**Figure 4.** Cross sections through the 3D NMR data along the  $F_2/F_3$  axis showing the coupling patterns for the methylene protons marked A and B in Figure 3.

inal coupling and a 10-Hz vicinal coupling, while the upfield geminal proton appears to be only split by its geminal neighbor. The vicinal coupling reflects averaging of the rotational isomeric states in solution and depends on the population of the trans (11 Hz) and gauche (2 Hz) states. Vicinal couplings of 10 and 3 Hz are expected for a population of rotational isomers that are 90% trans. The 3-Hz coupling is not observed in Figure 4B presumably because the coupling is on the order of the line width and cannot be resolved. The 3D analysis shows a larger fraction of trans isomers than obtained from a line-shape analysis of the 1D NMR spectrum at 85 °C.<sup>12</sup>

The 3D NMR experiments presented here show a new method for the analysis of polymer chain conformation. This approach makes it possible to measure coupling information and chain conformation that is obscured by peak overlap and the broad lines commonly encountered in the NMR spectra of high polymers. However, it is limited in part by computer software and the digital resolution. With the advent of more sophisticated NMR spectrometers and computers, higher digital resolution spectra can be obtained to reduce the artifacts, such as distortions in the peak intensities. This will make it possible to measure coupling patterns for each stereo-

sequence that can be resolved in a 2D NOE experiment.<sup>6</sup> We are using this approach along with solid-state NMR and thermal analysis to explore the role of chain conformation in the properties of poly(vinyl acetate/vinylidene cyanide) films, and the complete results will be reported elsewhere.

**Acknowledgment.** We are grateful to Takeo Furukawa for the generous gift of the poly(vinyl acetate/vinylidene cyanide) used in these studies.

## References and Notes

- (1) Bovey, F. A. *Chain Structure and Conformation of Macromolecules*; Academic Press: New York, 1982.
- (2) Bovey, F. A.; Winslow, F. H. *Macromolecules. An Introduction to Polymer Science*; Academic Press: New York, 1979.
- (3) Bovey, F. A. *Nuclear Magnetic Resonance Spectroscopy*; Academic Press: New York, 1988.
- (4) Wüthrich, K. *NMR of Proteins and Nucleic Acids*; Wiley-Interscience Publications: New York, 1986.
- (5) Bax, A. *Two-Dimensional NMR in Liquids*; D. Reidel Publishing Co.: Boston, 1982.
- (6) Bovey, F. A.; Mirau, P. A. *Acc. Chem. Res.* **1988**, *21*, 37.
- (7) Schilling, F. C.; Bovey, F. A.; Bruch, M. D.; Kozlowski, S. A. *Macromolecules* **1985**, *18*, 1418.
- (8) Bank, A.; Leffingwell, J.; Thies, C. *Macromolecules* **1971**, *4*, 43.
- (9) Chûjô, R. *Makromol. Chem., Macromol. Symp.* **1988**, *20*, 183.
- (10) Inoue, Y.; Kawaguchi, K.; Maruyama, Y.; Jo, Y. S.; Chûjô, R.; Seo, I.; Kishimoto, M. *Polymer* **1989**, *30*, 698.
- (11) Jo, Y. S.; Inoue, Y.; Chujo, R.; Saito, K.; Miyata, S. *Macromolecules* **1985**, *18*, 1850.
- (12) Jo, Y. S.; Sakurai, M.; Inoue, Y.; Chujo, R.; Tasaka, S.; Miyata, S. *Polymer* **1987**, *28*, 1583.
- (13) Griesinger, C.; Sorensen, O. W.; Ernst, R. R. *J. Am. Chem. Soc.* **1987**, *109*, 7228.
- (14) Griesinger, C.; Sorensen, O. W.; Ernst, R. R. *J. Magn. Reson.* **1987**, *73*, 574.
- (15) Vuister, G. W.; Boelens, R.; Kaptein, R. *J. Magn. Reson.* **1988**, *80*, 176.
- (16) Vuister, G. W.; Boelens, R. *J. Magn. Reson.* **1987**, *73*, 328.
- (17) Jeener, J.; Meier, B. H.; Bachmann, P.; Ernst, R. R. *J. Chem. Phys.* **1979**, *71*, 4546.
- (18) Aue, W. P.; Karhan, J.; Ernst, R. R. *J. Chem. Phys.* **1976**, *63*, 4226.
- (19) Mirau, P. A.; Heffner, S. A.; Bovey, F. A. *J. Magn. Reson.*, in press.
- (20) States, D. J.; Haberkorn, R. A.; Ruben, D. J. *J. Magn. Reson.* **1982**, *48*, 286.

Peter A. Mirau,\* Sharon A. Heffner, and Frank A. Bovey

AT&T Bell Laboratories, Room 1A-256  
600 Mountain Avenue, Murray Hill, New Jersey 07974

Received May 10, 1990

Revised Manuscript Received July 12, 1990